ELSEVIER

# Latrunculin B effects on trabecular meshwork and corneal endothelial morphology in monkeys ☆

Ilana Sabanay[a], Baohe Tian[b], B'Ann T. Gabelt[b], Benjamin Geiger[a], Paul L. Kaufman[b,*]

[a]*Department of Molecular Cell Biology, Weizmann Institute of Science, Rehovot, Israel*
[b]*Department of Ophthalmology and Visual Sciences, University of Wisconsin, Madison, F4/328 CSC, 600 Highland Avenue, Madison, WI 53792-3220, USA*

## Abstract

To determine the mechanism of latrunculin B (LAT-B)-induced decrease in outflow resistance and the effect of LAT-B on the cornea, structural changes of the trabecular meshwork (TM) and the corneal endothelium following LAT-B were studied in the live monkey eye. LAT-B (0.5 μM) and vehicle were administered by anterior chamber exchange and infusion with cationized and non-cationized gold solution in opposite eyes. The eyes were fixed by infusing Ito's solution and enucleated. Anterior segments were quadrisected and embedded in Epon-Embed 812. Morphology of the TM and the corneal endothelium was studied by light and electron microscopy. LAT-B-induced morphological changes in the TM included: (1) loss of microfilament integrity in cells, especially in TM cells on the collagen beams; (2) development of numerous cytoplasmic projections of the sub-canalicular cells (SUB); (3) reorganization of intermediate filaments in Schlemm's canal inner wall (IW) cells; (4) massive 'ballooning' of the juxtacanalicular (JXT) region, leading to a substantial expansion of the space between the IW of Schlemm's canal and the trabecular collagen beams; and (5) retention of extracellular matrix (ECM), trapped between the SUB cell layer and IW cells. No detrimental effects on tight junctions, giant vacuoles, and cell–cell and cell–ECM adhesions were observed. Endocytosis of gold particles was not affected. Morphology of the corneal endothelium of the LAT-B-treated eye was unchanged. In conclusion, TM changes in the LAT-B-treated eye suggest that the expansion of the JXT space may account for the decrease in outflow resistance induced by latrunculins. The outflow-effective concentration of LAT-B administered intracamerally does not significantly affect the corneal endothelium.
© 2005 Elsevier Ltd. All rights reserved.

*Keywords:* corneal endothelium; cytoskeleton; latrunculin B; monkey eye; trabecular meshwork

## 1. Introduction

The marine macrolides latrunculins, isolated from the ocean sponge *Negombata* (formerly *Latrunculia*) *magnifica*, are specific and potent actin-disrupting agents that sequester monomeric G-actin, leading to the disassembly of actin filaments (Coué et al., 1987; Lyubimova et al., 1997;

Spector et al., 1983; Spector et al., 1989). Latrunculins A and B (LAT-A and B) are the two common latrunculins which cause reversible dose- and time-dependent destruction of actin bundles and associated proteins in several types of cultured cells including human trabecular meshwork (TM) cells (Cai et al., 2000; Epstein etal., 1999). In living monkeys, both LAT-A and LAT-B increase outflow facility and decrease intraocular pressure (IOP) (Epstein et al., 1999; Okka et al., 2004; Peterson et al., 1999, 2000a), probably by directly reducing outflow resistance in the TM. The relevant mechanism of latrunculin-induced resistance decrease in the outflow pathway has been attributed to disruption of the actin cytoskeleton in TM and Schlemm's canal (SC) cells (Cai et al., 2000; Epstein et al., 1999; Peterson et al., 1999). However, the actual structural changes in the TM induced by latrunculins are still unknown. Morphological studies of the conventional drainage pathway following latrunculins are needed to

clarify the mechanism of the drug-induced increase in outflow facility, which might facilitate the development of specific target-selective cytoskeletal anti-glaucoma therapy. Additionally, studies of the morphology of the corneal endothelium are also important for safety consideration. Since LAT-B is 10 times more potent in reducing outflow resistance than LAT-A (Peterson et al., 1999, 2000a) and has fewer and milder adverse effects (Peterson et al., 2000b), we used LAT-B in this study. We perfused the AC of opposite eyes of live cynomolgus monkeys with fluid containing a mixture of cationized and non-cationized colloidal gold±LAT-B, while measuring the outflow rate. Morphology of the TM, SC and the corneal endothelium, and the fine distribution of the gold particles in the TM were studied by light and electron microscopy (LM, EM) after perfusion.

## 2. Materials and methods

### 2.1. Animals and anaesthesia

Two normal young adult cynomolgus monkeys (*Macaca fascicularis*), weighing ∼4 kg, were studied in accordance with UW and NIH guidelines, and with the ARVO Statement on the Use of Animals in Ophthalmic and Vision Research. Both monkeys (K554 and K596) had not received any prior invasive ocular procedures; all were free of AC cells and flare by slit-lamp biomicroscopy. Anaesthesia was induced with i.m. ketamine (10 mg/kg) followed by i.v. pentobarbital-Na (15 mg/kg).

### 2.2. Chemicals and drug preparation

LAT-B was obtained from Calbiochem–Novabiochem International, Inc., La Jolla, CA and stored as a 2 mM stock solution in DMSO (dimethyl sulfoxide; Sigma Chemical Co., St. Louis, MO) at −20°C. Cationic colloidal gold (5 nm particles; $5 \times 10^{13}$ particles/ml in 20% glycerol) and bovine serum albumin (BSA)-conjugated gold (10 nm particles; $5.7 \times 10^{12}$ particles/ml in 20% glycerol+1% BSA; optical density=3.13 at 520 nm) were from British BioCell International, Ltd, distributed by Ted Pella, Inc, Redding, CA. BSA-conjugated gold was dialysed before use against 400 ml×2 changes of Bárány's solution (a phosphate-based buffer used as mock aqueous humour in AC perfusion studies) (Bárány, 1964). The perfused gold solution comprised Bárány's solution and equal concentrations (particles/ml) of cationized gold (5 nm particles) and dialysed non-cationized gold (10 nm particles) conjugated to albumin. LAT-B (0.5 μM) or vehicle solution was prepared with the gold solution plus 0.5% DMSO (pH: ∼7).

### 2.3. Gold±LAT-B infusion

Before infusion with gold±LAT-B solution in opposite eyes, baseline outflow facility were determined by two-level constant pressure (25/35 mmHg) perfusion of the AC with Bárány's solution from an external reservoir (Bárány, 1964, 1965). This measurement would assure that the conventional outflow pathways of two eyes of each animal were functionally normal and reasonably similar at the start. The pressures were ∼25/35 mmHg rather than ∼15/25 mmHg as in previous physiological studies (Tian et al., 1998), because perfusion at the higher pressures would determine if the experimental animals had similar resistance washout in both eyes during the short period before drug administration (monkeys whose overall outflow rate/facility in one eye differed from averaged outflow rate/facility in both eyes by 10% or more were not selected for the morphological study). Since previous studies had shown that LAT-B significantly increased perfusion outflow facility in living monkeys (Okka et al., 2004; Peterson et al., 2000a), we did not replicate those findings in the morphological study to minimize resistance washout and any related structural changes. However, to obtain physiological evidence of drug potency and efficacy before launching the structural studies in the monkey eye, post-drug or vehicle outflow rate (assumed to be represented by the rate of fluid flow from the reservoir to the eye) was measured during gold±LAT-B infusion (for 15 [K554] or 25 min [K596]) at 25 mmHg. Although the measured outflow rate did not include aqueous humour formation, it would not affect the relevant result because LAT-B would not significantly alter aqueous humour formation (Peterson et al., 2000b) and the drug-induced changes in outflow rate were obtained by comparing outflow rates in contralateral eyes that were assumed to have similar and stable aqueous humour formation.

Briefly, the AC of both eyes was cannulated with a branched needle connected to a reservoir (inflow line) and pressure transducer and an unbranched needle with tubing clamped off. Following 35-min baseline outflow measurement, the clamped tubing from the unbranched needle was connected to syringes containing 0.5 μM LAT-B/vehicle solution (gold±LAT-B) in contralateral eyes. The syringes were placed in a variable speed infusion pump and the inflow line was disconnected and opened to air as a temporary outflow line, allowing infusion of 2 ml of gold±LAT-B solution through the AC for ∼12 min (∼0.17 ml/min), maintaining IOP at ∼10–15 mmHg. The reservoirs were emptied and filled with the identical solution as perfused through the eye. After the AC exchange, the inflow line was reconnected to the reservoir and the syringe tubing was clamped again. The reservoirs were then closed for the next 30 min without external fluid flowing into the eyes, and then re-opened, so that gold±LAT-B solution flowed into each eye for 15 or 25 min at 25 mmHg, while outflow rate was determined. Following the infusion with
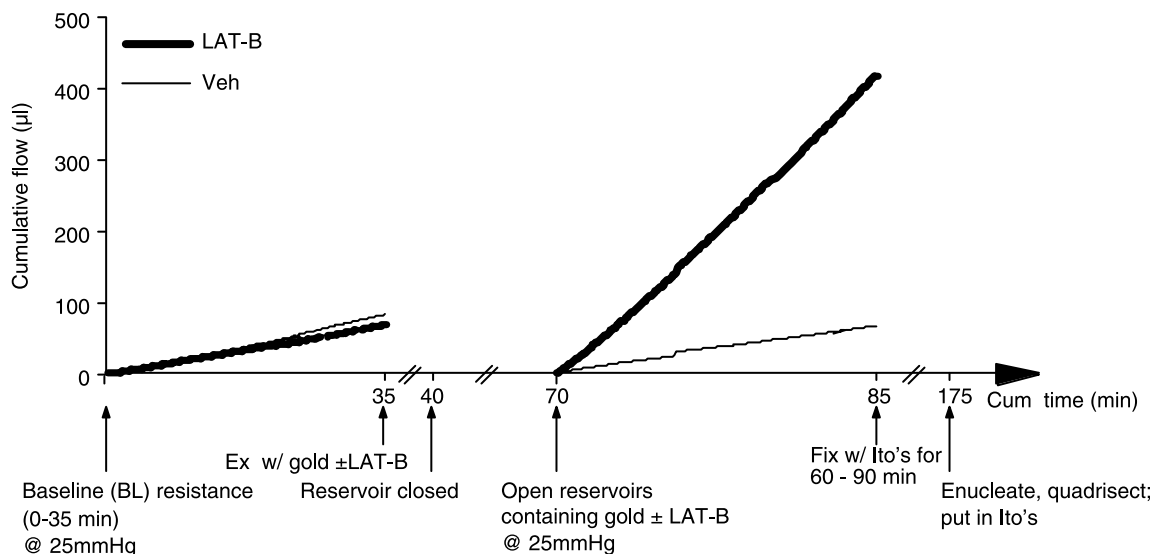
Fig. 1. Time track for monkey eye preparations and outflow (μl/min) before and after anterior chamber exchange (Ex) with 0.5 μM LAT-B or vehicle in a cynomolgus monkey (K554). Contralateral baseline outflow rates are not significantly different. Post-drug outflow rate is substantially higher in the LAT-B-treated eye than in the vehicle-treated eye.

gold±LAT-B solution, the inflow tubing was switched to reservoirs containing Ito's fixative (formaldehyde–glutaraldehyde fixatives) (Ito and Karnovsky, 1968) that was allowed to flow into the eyes for 60–90 min at 25 mmHg (Fig. 1).

Before perfusions, the femoral artery and vein of each monkey were cannulated under ketamine + pentobarbital anaesthesia. During fixation with Ito's solution (beginning 40–45 min after Ito's flow into the eye), exsanguinations were conducted by infusing lactated Ringers solution through the femoral vein while letting blood flow out of the femoral artery. Blood pressure in the artery during exsanguinations was monitored and maintained at the original level by adjusting the flow of lactated Ringers solution.

### 2.4. LM and EM of the TM and the corneal endothelium

After fixation, both eyes were enucleated under supplemental pentobarbital anaesthesia just before euthanization by pentobarbital overdose. The anterior segment was quadrisected and placed in Ito's fixative and embedded in Epon- Embed 812 (Electron Microscopy Sciences, Fort Washington, PA). Specimens for LM were sectioned (0.5 μm) with an ultramicrotome (Leica Ultracut—UCT, Vienna, Austria), stained with Epoxy tissue stain (EMS, Fort Washington, PA), and photographed using a digital camera (Nikon E800, DXM1200, Tokyo, Japan). All four quadrants in all eyes were examined by LM. Only regions that showed no handling artefacts were examined by EM, usually 2–3 quadrants per specimen. Specimens for transmission EM were sectioned (700 Å) with the ultra-microtome, stained with uranyl acetate and lead citrate, examined with a transmission electron microscope (model

CM12; Philips, Eindhoven, Holland) and recorded with a SIS Biocam CCD, 1024×1024 pixel camera (Munster, Germany). Although the junction-to-junction (J–J) distance of a cell may not represent that cell's diameter (e.g. the J–J distance may show a full diagonal of a cell in some sections, but it may be shorter in others when cut close to the cell's edge), the mean J–J distance in randomly oriented sections still reflects the cell's general size. Therefore, we conducted the J–J distance measurement under the hypothesis that the distribution of such distances will shift to larger values when cells 'relax'. Measurement of J–J distances of the inner wall (IW) cells was performed using the analysis software (Soft Imaging System GmbH, Muenster, Germany), directly on the raw microscope images. All adherens junctions were marked manually, and the distance between marks was measured. The quantitative data were derived from extended regions along SC that were well preserved (encompassing >30 cells each). Other less extended areas were also examined, but not measured (>10 grids for every specimen, in different quadrants). Comparison of the J–J distances of IW cells between the LAT-B-treated eye and the vehicle-treated eye was made using the 2-tailed unpaired t-test for difference vs. 0.0.

## 3. Results

### 3.1. Outflow

Both monkeys had similar baseline outflow rate in both eyes, but post-drug outflow rate in the LAT-B-treated eye was substantially higher than that in the contralateral control eye (Fig. 1). This indicated that the increased outflow rate in the LAT-B-treated eye was due to the drug's effect rather

than just to the perfusion itself. Additionally, baseline outflow facilities in both eyes of the two monkeys were also very similar (e.g. overall baseline outflow facility in the LAT-B-treated vs. the control eye $= 0.15$ vs. $0.18$ μl/min/mmHg in K554 and $0.37$ vs. $0.31$ μl/min/mmHg in K596). This, in conjunction with the similar contralateral baseline outflow rates (e.g. overall baseline outflow rate in the LAT-B-treated vs. the control eye $= 4.4$ vs. $5.1$ μl/min in K554 and $7.3$ vs. $7.1$ μl/min in K596), provided evidence that the two monkeys in this study had similar resistance washout in opposite eyes before drug administration. This was a prerequisite for the morphological study to assure that resistance washout-related structural changes would not confound drug-induced changes in TM morphology when contralateral eyes were compared. Post-drug outflow facility was not measured in this study for the reasons described in the method section.

Although we selected 2 monkeys (K554 and K596) that had similar baseline resistance washout at the same pressures in opposite eyes, some comparisons in the TM morphology were made between the K554-drug-treated eye and the K596-vehicle-treated eye (see figure legends). Since the 2 monkeys were perfused at the same pressures, and since the K554-drug-treated eye had a lower outflow rate/facility than the K596-vehicle-treated eye (5.1 vs. 7.1 μl/min or 0.18 vs. 0.31 μl/min/mmHg), these comparisons should not alter the conclusions qualitatively (see Section 4).

### 3.2. TM morphology

By LM, the morphology of the vehicle-treated eye was completely normal (Fig. 2a), as previously described (Sabanay et al., 2000; Sabanay et al., 2004); the JXT space in the LAT-B-treated eye was substantially increased when compared to that in the vehicle-treated eye (Fig. 2b; compare to Fig. 2a). In the LAT-B-treated eye, SC appeared to be slightly dilated and the overall geometry of the corneoscleral region of the TM was essentially normal and apparently intact (Fig. 2b).

By EM, the morphology of the TM in both eyes was consistent with that in LM (Fig. 3). Cell–cell junctions between the IW cells were retained after LAT-B, as indicated by the appearance of the junctional complexes and the strict localization of the 'granular' material (formed by proteins in blood upon fixation) to the canal's lumen, without crossing the tight-junctional barrier (There was some blood in the SC, which occurs occasionally irrespective of treatment, and does not affect the morphology of the IW or other cells). The 'granular' material was useful for identifying the nature of apparent vesicles/ membrane infoldings. In Fig. 3a, the same granularity was seen inside some large 'vesicles' (in cross section) and the SC, suggesting that the 'vesicles' were, in fact, just membrane infoldings. In the LAT-B-treated eye, one of the most striking morphological changes was a massive
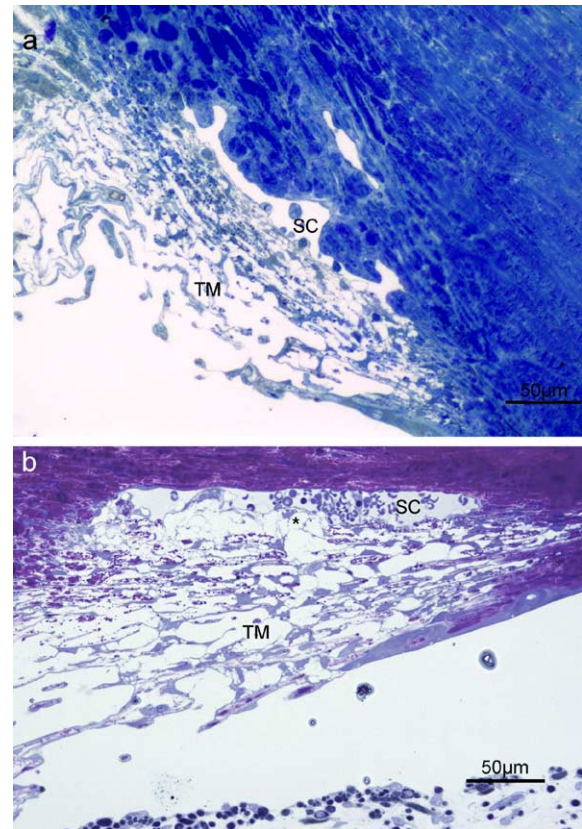


Fig. 2. LM of toluidine-blue-stained Epon sections of the trabecular meshwork (TM) following vehicle (a) or LAT-B (b). Panel (a) shows normal TM and Schlemm's canal (SC)(K554). Panel (b) indicates the increase of the juxtacanalicular space (asterisk) after LAT-B (K554).

'ballooning' of the JXT region, creating a wide space between the SUB cell layer and trabecular collagen beam meshwork (Fig. 3c; compare to Fig. 3b). Numerous thin and long cellular processes were formed by SUB cells, but not IW or outer wall cells. These processes were similar to those formed by a wide variety of cultured cells following latrunculins (Zimerman et al., 2004) and morphologically distinct from the physiological extensions formed by these cells in the vehicle-treated eye (Fig. 3b) (Sabanay et al., 2000). High magnification demonstrated the absence of organelles from these processes, the irregular diameter of these processes and the entrapment of ECM deposits in these altered intercellular spaces (Fig. 3d). The retention of close contact between IW and SUB cells was observed (Fig. 3a, c). Giant vacuoles (GV) were prominent in the LAT-B-treated eye (Fig. 3a), although it is difficult to state whether LAT-B increased GV prominence due to the apparent variability in the prominence of GV in the vehicle-treated eye (Fig. 3b), as well as their non-homogeneous distribution along the canal's wall (Fig. 3b).

In IW cells, high magnification images by EM revealed that LAT-B did not affect intercellular junctions, including tight junctions and adherens junctions (Fig. 4b vs. Fig. 4a). Cytoskeletal organization in the LAT-B-treated cells was
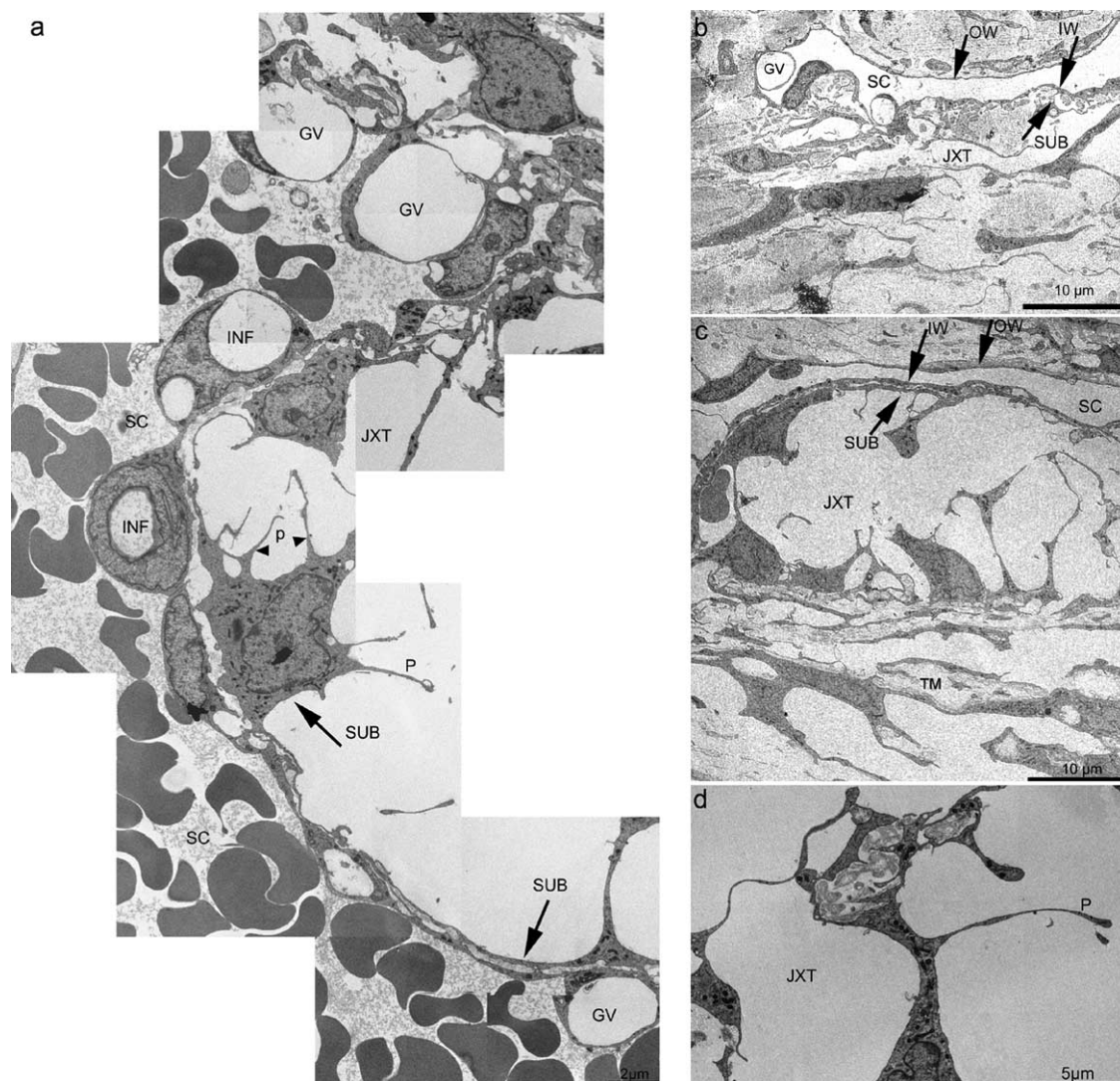
Fig. 3. Transmission EM of the trabecular meshwork (TM) following LAT-B (a, c and d [K554]) or vehicle (b [K596]). GV, giant vacuoles; INF, membrane infoldings; IW, inner wall; JXT, juxtacanalicular region; OW, outer wall; P, cellular processes; SC, Schlemm's canal; SUB, sub-canalicular cells. In (a), a long 'montage' of images is shown, depicting the IW - JXT regions of the TM following LAT-B. Panel (b) shows normal JXT region and its circumjacent structures; (c) indicates the massive 'ballooning' of the JXT region and the retention of close contact between IW and SUB (compare to (b)); (d) shows the absence of organelles from processes, irregular diameter of processes, and the entrapment of extracellular matrix deposits in intercellular spaces.

severely perturbed, manifested by the loss of alignment of intermediate filaments within the cells (Fig. 4d vs. Fig. 4c). LAT-B-induced changes in microfilaments might account for the perturbation of intermediate filaments, since cytoskeletal filaments are part of an interactive network so that affecting one system may have considerable indirect effects on the others. Cells in the LAT-B-treated eye were active in endocytosis, containing numerous gold-filled vesicles of different dimensions. These vesicles varied in their appearance, from clear to dark (ECM-filled) and from small ($\sim 50$ nm) single to multivesicular vesicles (Fig. 5b). However, in cells of the vehicle-treated eye, there were fewer gold-filled vesicles (Fig. 5a). Gold particles were mainly seen on ECM along the SUB-IW area in the LAT-B-treated eye but not in the vehicle-treated eye (Fig. 5d vs.

Fig 5c). Gold particles were also observed in the space of the SUB region, associated with ECM, and in caveoli as well as 'fenestrated vacuoles' in IW cells in the LAT-B-treated eye (Fig. 5f). Only a few gold particles were seen in the SUB space in the vehicle-treated eye (Fig. 5e).

Attachments of the TM cells to the beams in the LAT-B-treated eye were retained, although the cells were rounded up so that the area of attachment was less (Fig. 6b). Processes produced by these cells were largely similar to those formed by cells in the vehicle-treated eye (Fig. 6a). LAT-B had a strong effect on actin integrity, manifested by a fuzzy morphology of microfilaments (Fig. 6d), compared to their well-organized morphology in the vehicle-treated eye (Fig. 6c).

The J–J distances of IW cells in the LAT-B-treated eye were slightly but significantly greater than that in
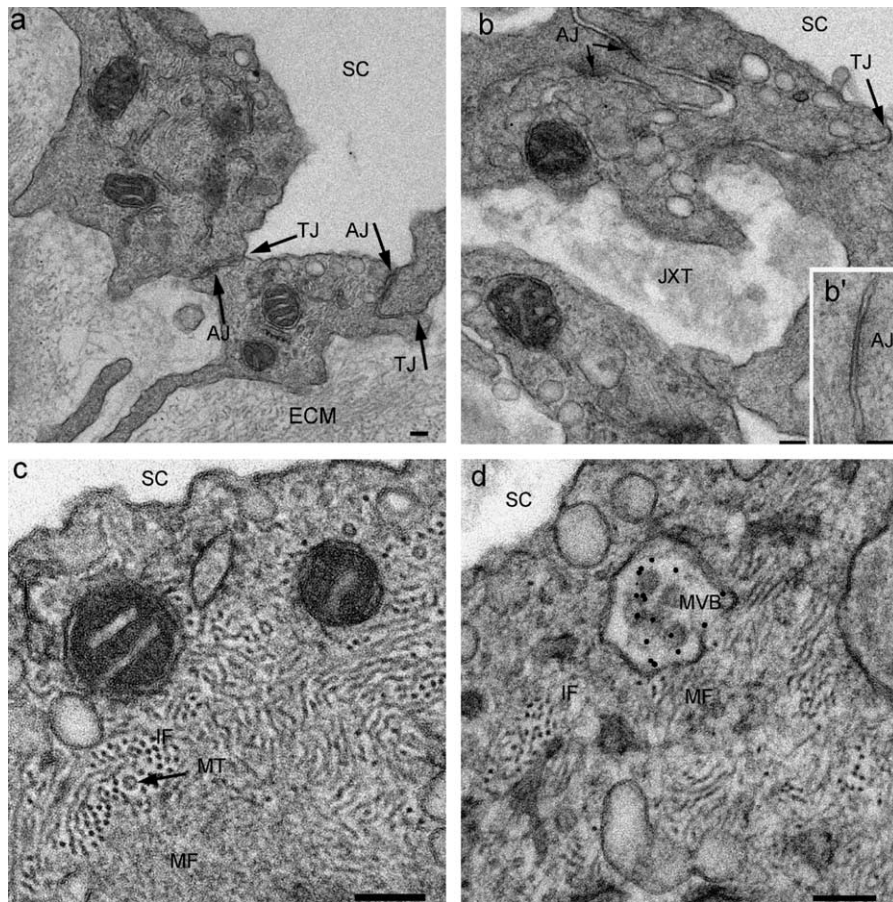
Fig. 4. Transmission EM of the inner wall of Schlemm's canal (SC) following vehicle (a, c [K596]) or LAT-B (b, d [K554]). AJ, adherens junctions; ECM, extracellular matrix; JXT, juxtacanalicular region; MF, microfilaments; MT, microtubules; MVB, multivesicular bodies; TJ, tight junctions. Panels (a) and (b) show intact intercellular junctions in both the vehicle-treated eye and the LAT-B - treated eye; (d) shows the loss of ordered alignment of intermediate filaments (IF) within the cells (compare to (c)). Bar =100 nm.

the vehicle-treated eye $(4.3 \pm 2.3\ \mu m$ vs. $3.1 \pm 1.9\ \mu m$; n1 =36; n2 =38, $P < 0.025$) (Fig. 7).

### 3.3. Corneal endothelium morphology

Morphology of the corneal endothelium after LAT-B was normal. Retention of all junctional elements, including tight junctions, adherens junctions and gap junctions, was noted in both the LAT-B-treated and the vehicle-treated eyes (Fig. 8).

## 4. Discussion

Previous studies have shown that LAT-B decreases outflow resistance in the living monkey eye and the enucleated porcine eye (Epstein et al., 1999; Peterson et al., 1999, 2000a). Since latrunculins depolymerize the polymeric actin (F-actin) by sequestering monomeric actin (G-actin), leading to changes in the cell shape and cell–cell adherens junctions in cultured cells (Coué et al., 1987; Lyubimova et al., 1997; Spector et al., 1983, 1989),

the LAT-B-induced decrease in outflow resistance during perfusion has been hypothesized to be due to TM/SC cell changes (Peterson et al., 1999, 2000a,b). The current morphological study has confirmed that LAT-B produces cytoskeletal disorganization in TM cells and IW cells of SC in vivo as it does in vitro (Cai et al., 2000; Epstein et al., 1999). However, the overall TM morphology after LAT-B is not quite consistent with the previous hypothesis. In the present study, LAT-B induces reorganization of the actin cytoskeleton in the TM and IW cells and the formation of numerous cytoplasmic projections of the SUB cells, and leads to a substantial expansion of the space between the IW of SC and the trabecular collagen beams. No detrimental effects on cellular junctions are observed. Among the morphological changes induced by LAT-B, the expansion of the JXT space may be the major structural basis for the drug to reduce outflow resistance, since it greatly enlarges the volume accessible to flow and increases the drainage surface. Although only two monkeys are studied based on the principle of sacrificing as few monkeys as possible, the data are clear and striking, and provide major new information.
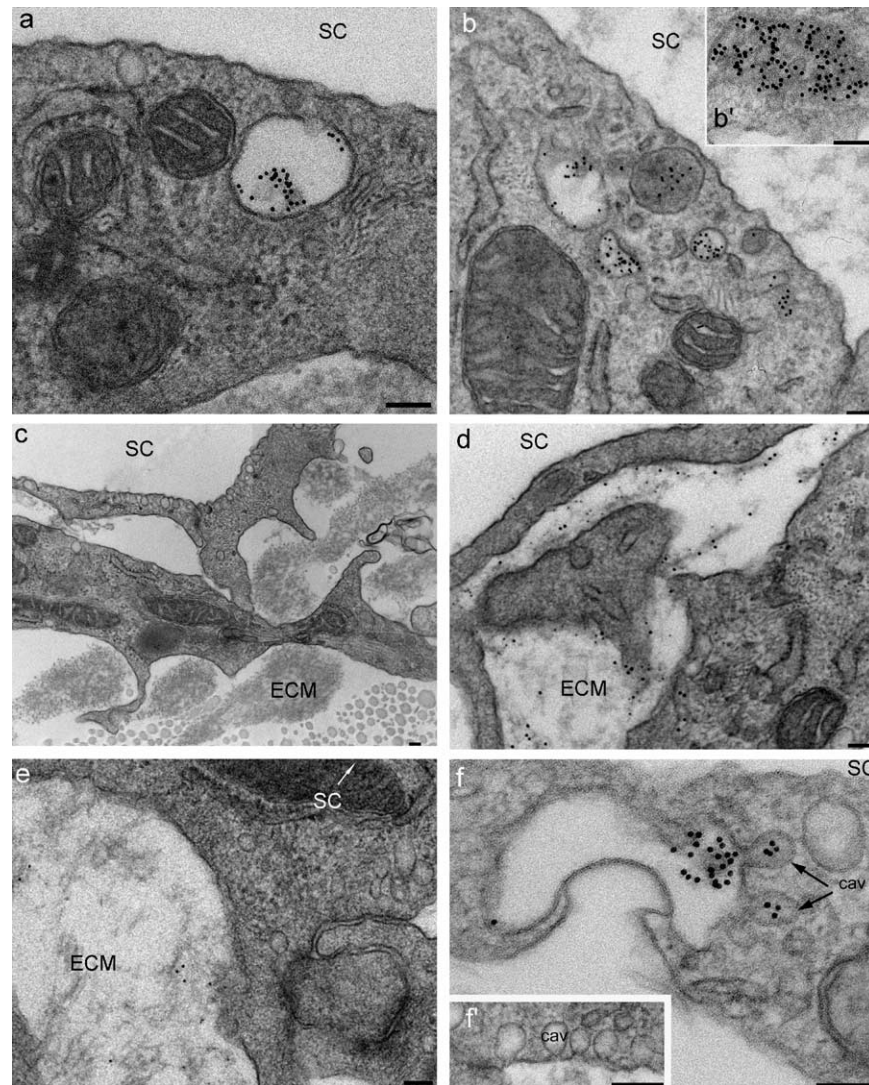
Fig. 5. Transmission EM of the inner wall of Schlemm's canal (SC) following vehicle (a, c, e [K596]) or LAT-B (b, d, f [K554]). Panel (b) shows numerous gold-filled vesicles of different dimensions in the LAT-B - treated eye (compare to (a)); (d) and (f) show gold particles in the sub-canalicular space or along the sub-canalicular and inner wall area, associated with ECM, or in caveoli (CAV) and 'fenestrated vacuoles' in inner wall cells in the LAT-B - treated eye. Panels (c) and (e) show fewer gold particles in the sub-canalicular and inner wall area in the vehicle-treated eye. Arrow in panel (e) indicates the direction of SC. Bar=100 nm.

The LAT-B-induced expansion of the JXT region is quite similar to the TM extension induced by pilocarpine, although the effect of the latter on the TM is indirect. Pilocarpine contracts the ciliary muscle, which 'spreads' or 'expands' the TM, JXT and SC by virtue of the muscle's attachments to these tissues and in turn reduces outflow resistance (Kaufman and Bárány, 1976). The reduced outflow resistance in the pilocarpine-treated monkey eye correlates best with the formation of apparently empty spaces in the sub-IW region (Lütjen-Drecoll, 1973). Unlike pilocarpine, LAT-B directly expands the JXT space perhaps by inhibiting contractility of TM cells. The current data and previous studies (Sabanay et al., 2000, 2004) suggest that under normal conditions the IW and JXT cells are in a contracted state and that reduction in their contractility can

expand these tissues and alter the routes and extent of fluid flow. Although LAT-B does not directly affect cellular contractility, the drug-induced F-actin depolymerization may secondarily induce cellular relaxation, since there is a close relationship between cellular contractility and the actin cytoskeleton (Burridge and Chrzanowska-Wodnicka, 1996; Chrzanowska-Wodnicka and Burridge, 1996). This is supported by a previous study where LAT-B relaxed the iris sphincter and ciliary muscle in living monkeys, with some separation of miotic and accommodative effects (Okka et al., 2004).

Several other cytoskeletal drugs, such as cytochalasin B, ethacrynic acid and H-7, also increase outflow facility in enucleated calf and human eyes and/or in living monkey eyes by directly reducing outflow resistance in the TM
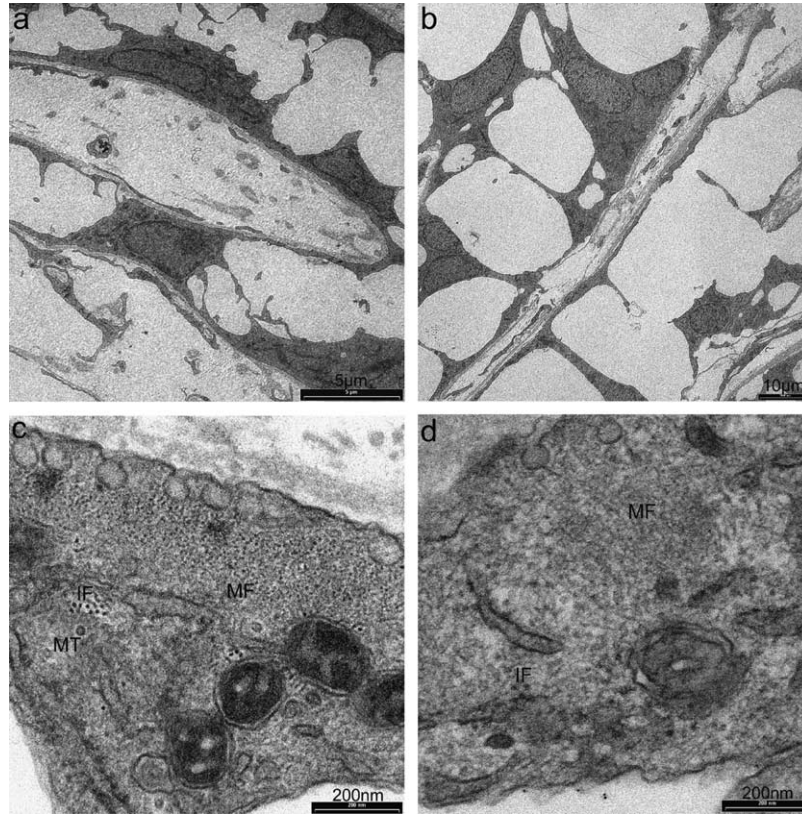
Fig. 6. Transmission EM of cells attached to the collagen beams in the trabecular meshwork of the vehicle-treated eye (a, c [K596]) and the LAT-B-treated eye (b, d [K554]). Cells in the LAT-B-treated eye (b) remained attached to the collagen beams. Processes produced by these cells are largely similar to those formed by cells in the vehicle-treated eye (compare a to b). Panel (d) shows a fuzzy appearance of microfilaments (MF), compared to (c). IF, intermediate filaments; MT, microtubules.
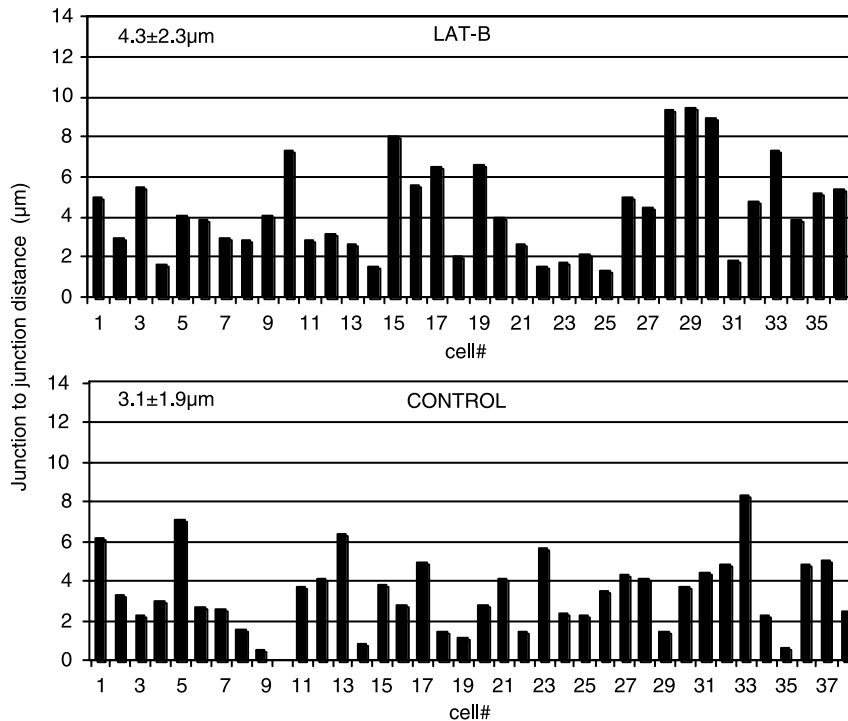


Fig. 7. Histogram showing the junction-to-junction distance of inner wall cells in the LAT-B-treated eye (K554) and the vehicle-treated eye (K554). The treatment with LAT-B induces an increase in mean junction-to-junction distance from $3.1 \pm 1.9$ μm to $4.3 \pm 2.3$ μm (n1 = 36; n2 = 38, $P < 0.025$).
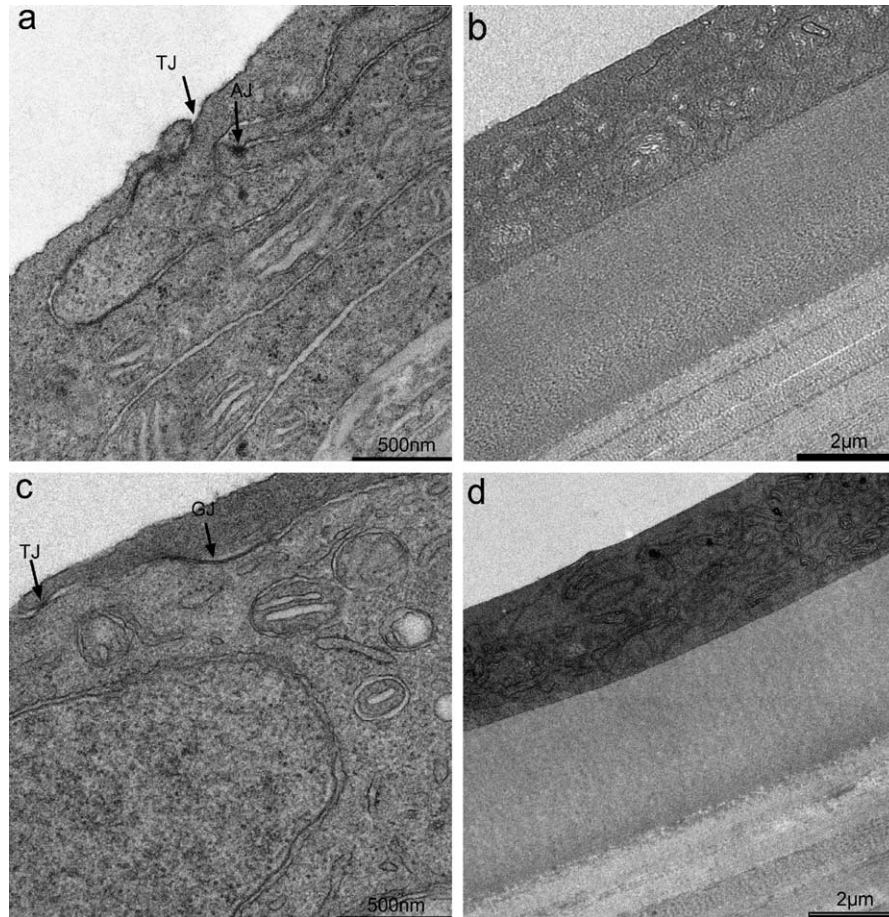
Fig. 8. Effect of LAT-B on corneal endothelium. (a, b), vehicle - treated eye (K596); (c, d), LAT-B-treated eye (K596). Note the retention of all junctional elements, including tight junctions (TJ), adherens junctions (AJ) and gap junctions (GJ), in the LAT-B-treated eye.

(Epstein et al., 1987; Svedbergh et al., 1978; Tian et al., 1998).

Cytochalasin B induces distension of the meshwork, separation of meshwork cells from one another, and breaks in the IW endothelium (Svedbergh et al., 1978). Lower resistance-effective doses of ethacrynic acid do not produce morphological changes in the TM, but higher doses induce separations between TM and IW cells (Liang et al., 1992). Cell–cell separation may be one of the mechanisms by which these drugs decrease outflow resistance, but it may also be the cause of the drug-induced damage to the corneal endothelium. Unlike cytochalasin B and ethacrynic acid, LAT-B does not induce cell–cell separations in the live monkey eye as seen by transmission EM, although it disrupts human TM cell–cell junctions in culture (Epstein et al., 1999). The absence of apparent cell–cell separations may suggest that the cellular contacts in vivo are more stable than those formed in vitro, so that LAT-B effects on the cells in vivo are subtler than those reported in vitro. Although transmission EM, compared to scanning EM, may have limitations in revealing the occurrence and frequency of changes in cell–cell junctions (e.g. changes in cell border

pores of IW cells that account for only about 0.1% of the total IW area, so that the chances of cutting through a paracellular pore are less), the substantial increase in outflow rate following LAT-B (Fig. 1) likely cannot be explained by rare or minor changes in cell–cell junctions alone. Further studies by scanning EM are needed to clarify this issue. Additionally, different concentrations of the drug may nave different effects on cell–cell junctions. Although it is unknown if higher doses of LAT-B will affect the TM differently in the live monkey eye, the resistance-effective LAT-B dose used in this study further indicates that cell–cell separation is not indispensable for the resistance decrease. The JXT space expansion without meaningful detrimental changes in cellular junctions may be a favourable strategy to reduce outflow resistance from a safety perspective.

The H-7-induced decrease in outflow resistance is associated with expansion of the intercellular spaces in the JXT meshwork, accompanied by removal of ECM. The IW cells of SC become highly extended, yet cell–cell junctions are maintained (Sabanay et al., 2000, 2004). The major differential effect of LAT-B on the TM morphology

compared to H-7 is that the former induces separation between the SUB cells and the rest of the JXT tissue, rather than between IW and JXT cells as seen after latter (Sabanay et al., 2000). Additionally, expansion of the canal's wall after LAT-B is significant, yet considerably smaller than that observed after H-7 (Sabanay et al., 2000). The absence of a substantial change in cellular contractility in the IW cells after LAT-B may prevent SUB cell detachment from the SC, so that the ECM between the two cell layers cannot be released into the expanded JXT region or washed away into the canal's lumen through the IW, and thus the JXT region expansion occurs between the SUB cells and the collagen beams. However, both LAT-B and H-7 induce expansion of the JXT space without apparently affecting cell–cell junctions in the TM and IW cells. This phenomenon, in conjunction with the TM changes induced by the indirect effect of pilocarpine, suggests that the major outflow resistance in the TM may be at the JXT region as described in previous studies (Bill and Svedbergh, 1972; Ethier et al., 1986; Maepea and Bill, 1992; Seiler and Wollensak, 1985) and that the change of overall geometry of the JXT region may be one of the most important mechanisms in the outflow resistance decrease.

High pressures during perfusion might induce pressure-dependent structural changes in the TM, including simple pressure-induced changes and pressure-dependent drug-induced changes. The simple pressure-induced TM changes should not affect the conclusions based on the comparison between opposite eyes, because the latter were perfused simultaneously at the same pressure and had similar resistance washout during perfusion. Even though some comparisons were made between the drug-treated eye and the vehicle-treated eye from different monkeys in the present study, it should not alter the conclusions qualitatively, since the two eyes were perfused at the same pressure and the drug-treated eye had smaller baseline resistance washout than the vehicle-treated eye. If any resistance washout-related TM change occurs, these comparisons might only attenuate, rather than exaggerate, the drug-induced changes in the TM. The pressure of 25 mmHg was a reasonable compromise to effectively deliver gold particles and fixative into the TM while minimizing pressure-induced structural changes. Additionally, although we did not determine the LAT-B-induced morphological changes in the TM at different pressures, we may still speculate that high pressures enhance the drug's effects on the TM, since cytoskeletal drug-induced decrease in outflow resistance is pressure-dependent (Peterson et al., 1999; Peterson et al., 2000a; Sabanay et al., 2000). This phenomenon suggests that the effect of LAT-B on the TM may be more significant in the glaucomatous eye with elevated IOP.

Unlike a previous study using cationized and non-cationized ferritin in human anterior segments (Ethier and Chan, 2001), no consistent difference was found between distributions of cationized and non-cationized gold particles in any eye. Although the cationized gold may be a better flow tracer and the non-cationized gold attaches more readily to the ECM, both are primarily associated with ECM and vesicles. Gold particles are mainly seen on ECM along the SUB-IW area in the LAT-B-treated eye, but not in the vehicle-treated eye. It is not clear where the major gold particles in the vehicle-treated eye are; they are expected to be fewer than in the LAT-B-treated eyes, since less fluid is infused in the vehicle-treated eyes because of their higher flow resistance. The gold particles might be retained or distributed somewhere in the trabecular meshwork compartment, but large aggregates were not apparent. Although the findings do not inform about specific flow pathways through the meshwork, they further support the hypothesis that the major resistance reduction in the LAT-B-treated eye occurs in the JXT area. Further studies are needed to clarify this issue. The excellent internalization of the gold particles in the IW cells of the LAT-B-treated eye suggests that LAT-B does not block endocytosis in the TM.

It is worth noting that although LAT-B changes the TM morphology and reduces outflow resistance, it does not significantly affect the corneal endothelium. This is a very important feature for a potential anti-glaucoma medication. A possible explanation for the different effects of the drug on the TM and the cornea could be that the TM is a suspended multilayered tissue, in which JXT cells have no real basement membrane. When the actin cytoskeleton is disrupted by LAT-B, the TM can be readily distorted and distended by fluid flow down the pressure gradient between the AC and SC. However, the corneal endothelium in the live monkey eye is a single cell layer on a well defined solid basement membrane and ECM structure (Descemet's membrane and stroma) with much less fluid flow across it than the TM, and thus less easily distended or distorted even when the contractile apparatus, and consequently, cellular adhesions are weakened.

In conclusion, LAT-B used in this study reduces outflow resistance primarily by inducing JXT space expansion without adversely affecting the cornea. Therefore, expanding the JXT area available for fluid drainage, by relaxation of the JXT tissue either physiologically or pharmacologically using compounds such as LAT-B, may be a possible approach to glaucoma therapy.

# References

Bárány, E.H., 1964. Simultaneous measurement of changing intraocular pressure and outflow facility in the vervet monkey by constant pressure infusion. Invest. Ophthalmol. 3, 135–143.

Bárány, E.H., 1965. Relative importance of autonomic nervous tone and structure as determinants of outflow resistance in normal monkey eyes (Cercopithecus ethiops and Macaca irus). In: Rohen, J. W. (Ed.), The Structure of the Eye, Second Symposium. Schattauer, Stuttgart, pp. 223–236.

Bill, A., Svedbergh, B., 1972. Scanning electron microscopic studies of the trabecular meshwork and the canal of Schlemm: An attempt to localize the main resistance to outflow of aqueous humor in man. Acta Ophthalmol. 50, 295–320.

Burridge, K., Chrzanowska-Wodnicka, M., 1996. Focal adhesions, contractility, and signaling. Ann. Rev. Cell Devel. Biol. 12, 463–518.

Cai, S., Liu, X., Glasser, A., Volberg, T., Filla, M., Geiger, B., Kaufman, P. L., 2000. Effect of latrunculin-A on morphology and actin-associated adhesions of cultured human trabecular meshwork cells. Mol. Vision 6, 132–143 http://www.molvis.org/molvis/v6/a18/.

Chrzanowska-Wodnicka, M., Burridge, K., 1996. Rho-stimulated contractility drives the formation of stress fibers and focal adhesions. J. Cell Biol. 133, 1403–1415.

Coué, M., Brenner, S.L., Spector, I., Korn, E.D., 1987. Inhibition of actin polymerization by latrunculin A. FEBS Lett. 213, 316–318.

Epstein, D.L., Freddo, T.F., Bassett-Chu, S., Chung, M., Karageuzian, L., 1987. Influence of ethacrynic acid on outflow facility in the monkey and calf eye. Invest. Ophthalmol. Vis. Sci. 28, 2067–2075.

Epstein, D.L., Rowlette, L.L., Roberts, B.C., 1999. Acto-myosin drug effects and aqueous outflow function. Invest. Ophthalmol. Vis. Sci. 40, 74–81.

Ethier, C.R., Chan, D.W.H., 2001. Cationic ferritin changes outflow facility in human eyes whereas anionic ferritin does not. Invest. Ophthalmol. Vis. Sci. 42, 1795–1802.

Ethier, C.R., Kamm, R.D., Palaszewski, B.A., Johnson, M.C., Richardson, T.M., 1986. Calculations of flow resistance in the juxtacanalicular meshwork. Invest. Ophthalmol. Vis. Sci. 27, 1741–1750.

Ito, S., Karnovsky, M.J., 1968. Formadehyde-glutaraldehyde fixatives containing trinitro compounds.. J. Cell Biol. 39, 168a.

Kaufman, P.L., Bárány, E.H., 1976. Loss of acute pilocarpine effect on outflow facility following surgical disinsertion and retrodisplacement of the ciliary muscle from the scleral spur in the cynomolgus monkey. Invest. Ophthalmol. 15, 793–807.

Liang, L.L., Epstein, D.L., de Kater, A.W., Shahsafaei, A., Erickson-Lamy, K.A., 1992. Ethacrynic acid increases facility of outflow in the human eye in vitro. Arch. Ophthalmol. 110, 106–109.

Lütjen-Drecoll, E., 1973. Structural factors influencing outflow facility and its changeability under drugs. Invest. Ophthalmol. 12, 280–294.

Lyubimova, A., Bershadsky, A.D., Ben-Ze'ev, A., 1997. Autoregulation of actin synthesis responds to monomeric actin levels. J. Cell Biol. 65, 469–478.

Maepea, O., Bill, A., 1992. Pressures in the juxtacanalicular tissue and Schlemm's canal in monkeys. Exp. Eye Res. 54, 879–883.

Okka, M., Tian, B., Kaufman, P.L., 2004. Effect of low-dose latrunculin B on anterior segment physiologic features in the monkey eye. Arch. Ophthalmol. 122, 1482–1488.

Peterson, J.A., Tian, B., Bershadsky, A.D., Volberg, T., Gangnon, R.E., Spector, I., Geiger, B., Kaufman, P.L., 1999. Latrunculin-A increases outflow facility in the monkey. Invest. Ophthalmol. Vis. Sci. 40, 931–941.

Peterson, J.A., Tian, B., Geiger, B., Kaufman, P.L., 2000a. Effect of latrunculin-B on outflow facility in monkeys. Exp. Eye Res. 70, 307–313.

Peterson, J.A., Tian, B., McLaren, J.W., Hubbard, W.C., Geiger, B., Kaufman, P.L., 2000b. Latrunculin effects on intraocular pressure, aqueous humor flow and corneal endothelium. Invest. Ophthalmol. Vis. Sci. 41, 1749–1758.

Sabanay, I., Gabelt, B.T., Tian, B., Kaufman, P.L., Geiger, B., 2000. H-7 effects on structure and fluid conductance of monkey trabecular meshwork. Arch. Ophthalmol. 118, 955–962.

Sabanay, I., Tian, B., Gabelt, B.T., Geiger, B., Kaufman, P.L., 2004. Functional and structural reversibility of H-7 effects on the conventional aqueous outflow pathway in monkeys. Exp. Eye Res. 78, 137–150.

Seiler, T., Wollensak, J., 1985. The resistance of the trabecular meshwork to aqueous humor outflow. Graefes Arch. Clin. Exp. Ophthalmol. 223, 88–91.

Spector, I., Shochet, N.R., Blasberger, D., Kashman, Y., 1989. Latrunculins-novel marine macrolides that disrupt microfilament organization and affect cell growth: comparison with cytochalasin D. Cell Motil. Cytoskeleton. 13, 127–144.

Spector, I., Shochet, N., Kashman, Y., Groweiss, A., 1983. Latrunculins: novel marine toxins that disrupt microfilament organization in cultured cells. Science 219, 493–495.

Svedbergh, B., Lütjen-Drecoll, E., Ober, M., Kaufman, P.L., 1978. Cytochalasin-B induced changes in the anterior ocular segment of the cynomolgus monkey. Invest. Ophthalmol. Vis. Sci. 17, 1978.

Tian, B., Kaufman, P.L., Volberg, T., Gabelt, B.T., Geiger, B., 1998. H-7 disrupts the actin cytoskeleton and increases outflow facility. Arch. Ophthalmol. 116, 633–643.

Zimerman, B., Volberg, T., Geiger, B., 2004. Early molecular events in the assembly of the focal adhesion-stress fiber complex during fibroblast spreading. Cell Motil. Cytoskel. 58, 143–159.